

# Magneto-infrared spectroscopy of Landau levels and Zeeman splitting of three-dimensional massless Dirac Fermions in $\text{ZrTe}_5$

R. Y. Chen<sup>†,1</sup>, Z. G. Chen<sup>†,2</sup>, X.-Y. Song,<sup>1</sup> J. A. Schneeloch,<sup>3</sup> G. D. Gu,<sup>3</sup> F. Wang,<sup>1,4,\*</sup> and N. L. Wang<sup>1,4,†</sup>

<sup>1</sup>International Center for Quantum Materials, School of Physics, Peking University, Beijing 100871, China

<sup>2</sup>National High Magnetic Field Laboratory, Tallahassee, Florida 32310, USA

<sup>3</sup>Condensed Matter Physics and Materials Science Department,  
Brookhaven National Lab, Upton, New York 11973, USA

<sup>4</sup>Collaborative Innovation Center of Quantum Matter, Beijing, China

We present a magneto-infrared spectroscopy study on a newly identified three-dimensional (3D) Dirac semimetal  $\text{ZrTe}_5$ . We observe clear transitions between Landau levels and their further splitting under magnetic field. Both the sequence of transitions and their field dependence follow quantitatively the relation expected for 3D *massless* Dirac fermions. The measurement also reveals an exceptionally low magnetic field needed to drive the compound into its quantum limit, demonstrating that  $\text{ZrTe}_5$  is an extremely clean system and ideal platform for studying 3D Dirac fermions. The splitting of the Landau levels provides a direct and bulk spectroscopic evidence that a relatively weak magnetic field can produce a sizeable Zeeman effect on the 3D Dirac fermions, which lifts the spin degeneracy of Landau levels. Our analysis indicates that the compound evolves from a Dirac semimetal into a topological line-node semimetal under current magnetic field configuration.

PACS numbers: 71.55.Ak, 78.20.-e, 71.70.Di

3D topological Dirac/Weyl semimetals are new kinds of topological materials that possess linear band dispersion in the bulk along all three momentum directions[1–7]. Their low-energy quasiparticles are the condensed matter realization of Dirac and Weyl fermions in relativistic high energy physics[8, 9]. These materials are expected to host many unusual phenomena[10–12], in particular the chiral and axial anomaly associated with Weyl fermions[3, 13–15]. It is well known that the Dirac nodes are protected by both time-reversal and space inversion symmetry. Since magnetic field breaks the time-reversal symmetry, a Dirac node may be split into a pair of Weyl nodes along the magnetic field direction in the momentum space [16–18] or transformed into line-nodes[17, 19]. Therefore, a Dirac semimetal can be considered as a parent compound to realize other topological variant quantum states. However, past 3D Dirac semimetal materials (e.g.  $\text{Cd}_3\text{As}_2$ ) suffer from the problem of large residual carrier density which requires very high magnetic field (e.g. above 60 Tesla) to drive them to their quantum limit[20, 21]. This makes it extremely difficult to explore the transformation from Dirac to Weyl or line-node semimetals. Up to now, there are no direct evidences of such transformations.

$\text{ZrTe}_5$  appears to be a new topological 3D Dirac material that exhibits novel and interesting properties. The compound crystallizes in the layered orthorhombic crystal structure, with prismatic  $\text{ZrTe}_6$  chains running along the crystallographic  $a$ -axis and linked along the  $c$ -axis via zigzag chains of Te atoms to form two-dimensional (2D) layers. Those layers stack along the  $b$ -axis. A recent *ab initio* calculation suggests that bulk  $\text{ZrTe}_5$  locates close to the phase boundary between weak and strong topological insulators [22]. However, more recent transport and ARPES experiments identify it to be a 3D Dirac semimetal with only one Dirac node at the  $\Gamma$  point [23]. Interestingly, a chiral magnetic effect associated with the transformation from a Dirac to Weyl semimetal was observed on

$\text{ZrTe}_5$  through a magneto-transport measurement [23]. Our recent optical spectroscopy measurement at zero field revealed clearly a linear energy dependence of optical conductivity, being another hallmark of 3D massless Dirac fermions [24].

In this letter, we present magneto-infrared spectroscopy study on  $\text{ZrTe}_5$  single crystals. We observe clear transitions between Landau levels and their further splitting under magnetic field. Both the sequence of transitions and their field dependence follow quantitatively the relation expected for 3D *massless* Dirac fermions. Furthermore, the measurement reveals an exceptionally low magnetic field (about 1 Tesla) needed to drive the compound into its quantum limit. Both facts demonstrate that  $\text{ZrTe}_5$  is an extremely clean system and ideal platform for studying 3D Dirac fermions. The presence of further splitting of Landau levels, which has never been observed in 2D massless Dirac fermions, e.g. graphene, provides direct evidence for the lifting of spin degeneracy of Landau levels, an effect being linked to the transformation from a Dirac semimetal to a line-node or Weyl semimetal. Our theoretical analysis indicates that the former one is more likely realized in the present magnetic field configuration.

Figure 1 shows the reflectance spectra under different magnetic field  $R(B)$  renormalized by the zero field reflectance  $R(0)$  in the far- and mid-infrared region. For the lowest magnetic field (1 T), a series of peaks could be clearly resolved, which keep growing more pronounced and shift to higher energies when the field strength  $B$  increases. In optical reflectance measurement, such peak features usually come from the interband transitions. Since these sharp peaks emerge in the reflectivity only by applying magnetic field, it is natural to connect them to the Landau quantization of 3D Dirac electrons. Thus the peaks should stem from electronic transitions connecting different Landau levels. Significantly, the first broad peak, which appears at the lowest energy, gradually split into four narrow peaks as  $B$  increases. This character is quite in-

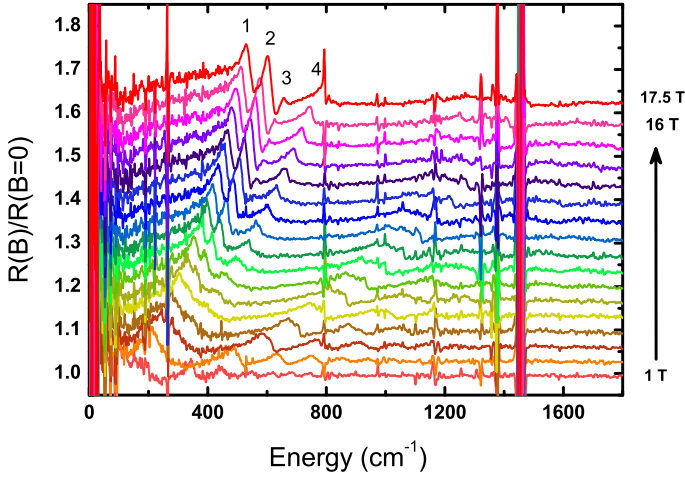


FIG. 1: The relative reflectivity of ZrTe<sub>5</sub> under magnetic field, as a function of energy. The spectrum are shifted upward by equal interval corresponding to different  $B$ .

triguing and has never been observed ever before, which will be explained in detail later. For the sake of convenience, they are marked by the numbers “1, 2, 3, 4” respectively at the top of Fig. 1. However, the splittings of other peaks located at higher energies are rather vague in this plot.

In order to verify our speculation on the origin of the emerging peaks and capture the underlying physics of 3D Dirac semimetal, we examine the sequence of peaks observed at low field. For a 3D system, the band structure would transform into a set of 1D Landau levels by applying strong enough magnetic field, which are only dispersive along the field direction. Theoretical calculation on an isolated Weyl point has suggested that the magneto-optical conductivity is constituted of a series of asymmetric peaks lying on top of a linear background [25, 26]. Especially, the peaks associated with allowed interband transitions in the Landau level structure occur at  $\omega \propto \sqrt{n} + \sqrt{n+1}$ , corresponding to transition from  $L_{-n}$  to  $L_{n+1}$  or from  $L_{-(n+1)}$  to  $L_n$ , where  $L_n$  represents for the  $n$ th Landau level. This conclusion applies to 3D massless Dirac fermion as well, because massless Dirac fermion can be thought as two sets of Weyl fermions with opposite chirality.

A linear rising optical conductivity has been revealed in our previous zero field spectroscopic experiment on ZrTe<sub>5</sub> single crystal [24] which already provides a strong evidence for 3D massless Dirac or Weyl fermions. We blew up the results of  $B = 2$  T as displayed in Fig. 2, in which six peaks could be clearly resolved. The positions of these peaks are identified to be about 202, 480, 628, 748, 856, 937 cm<sup>-1</sup> in sequence. The energy ratios of the peaks observed here can be approximately reduce to  $1 : 1 + \sqrt{2} : \sqrt{2} + \sqrt{3} : \sqrt{3} + \sqrt{4} : \sqrt{4} + \sqrt{5} : \sqrt{5} + \sqrt{6}$ , in nearly perfect accordance with the predicted massless Dirac semimetal behavior. This results in a linear dependence of the transition energy between Landau levels on  $\sqrt{n} + \sqrt{n+1}$ , as shown in the inset of the figure. From this observation, the first peak can be unambiguously determined

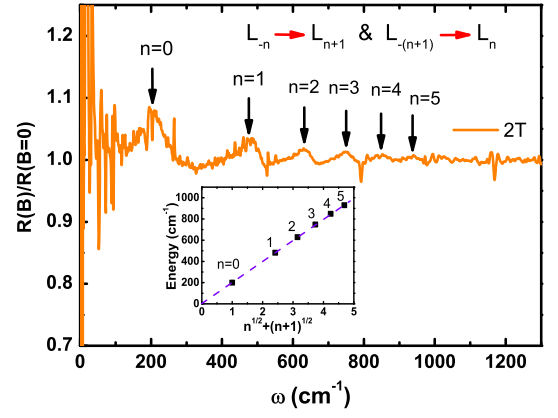


FIG. 2: The wave number dependent relative reflectivity  $R(B)/R(0)$  under magnetic field of 2 T.  $n = 0 \dots 5$  point to six different peaks in sequence. The inset shows the linear dependence of the transition energies between Landau levels on  $\sqrt{n} + \sqrt{n+1}$ . The dash line is a guide to the eyes.

to correspond to  $n=0$ , ascribed to transitions from  $L_0$  to  $L_1$  and  $L_{-1}$  to  $L_0$ . Only when the chemical potential lies in between  $L_1$  and  $L_{-1}$ , can this transition be clearly visible.[26] This is quite exciting because it demonstrates that the quantum limit could be easily approached by magnetic field as low as 1 T, where the  $n = 0$  peak is distinctively observed. As a contrast, the quantum limit of the well-known Dirac semimetal Cd<sub>3</sub>As<sub>2</sub> can not be reached with magnetic field lower than 65 T [20, 21]. It indicates that ZrTe<sub>5</sub> compound is extremely close to an ideal Dirac semimetal, with the chemical potential lying in the vicinity of Dirac point, and meanwhile it is an extraordinarily clean system. We anticipate that our finding of easy access of quantum limit will motivate many other experimental probes on this compound. In Supplemental Information [27] we perform more detailed analysis of this peak sequence and obtain estimates of the average  $ac$ -plane Fermi velocity  $v_{\perp} = \sqrt{v_a v_c} \sim 4.84 \times 10^5$  (m/s) and a vanishingly small Dirac mass  $|m| \sim 2$  (cm<sup>-1</sup>).

In Fig. 1, where  $R(B)/R(0)$  was shifted by equal interval with regard to increasing magnetic field, it is noted that the peak positions evolve in a way much alike the parabolic fashion as  $B$ . To further illustrate the characteristic features of the Landau levels, we plot  $R(B)/R(0)$  in a pseudo-color photograph as a function of  $\sqrt{B}$ . It is clearly seen in Fig. 3 that the wave numbers of the peaks are basically linear proportional to  $\sqrt{B}$ . The dashed lines are instructions for eyes, whose intercepts at 0 T are all absolute zero. For a single massless 3D Dirac node, the  $n$ th Landau levels caused by magnetic field are dispersive only along the field direction (see Supplementary Information[27] for more details), with doubly degenerate  $n \neq 0$  levels  $E_n(k_{\parallel}) = \text{sgn}(n) \cdot \sqrt{2v_{\perp}^2 eB\hbar \cdot |n| + \hbar^2 v_{\parallel}^2 k_{\parallel}^2}$ , and  $E_0(k_{\parallel}) = \pm \hbar v_{\parallel} k_{\parallel}$  for  $n = 0$ . If neglecting the dispersion along the magnetic field direction, then  $E_n \propto \sqrt{B}$ . As a comparison, for free electron systems, the magnetic induced Landau level obeys  $E_n = (n + \frac{1}{2})\hbar\omega_c$ , where  $\omega_c$  is the

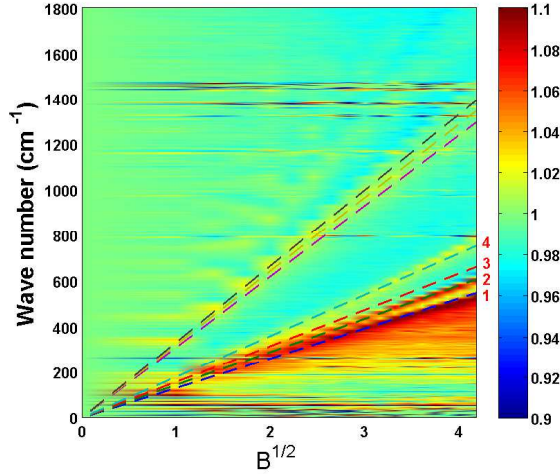


FIG. 3: The pseudo-colors photograph of the relative reflectivity  $R(B)/R(0)$  as functions of wave number and  $\sqrt{B}$ . The dashed lines are linear fittings of the peak energies dependent on  $\sqrt{B}$ .

cyclotron angular velocity and proportional to  $B$  instead of  $\sqrt{B}$ . Additionally, the Landau level energy of massive 3D Dirac fermions in topological insulator  $\text{Bi}_2\text{Se}_3$  is reported to be in linear scale with  $B$  as well[28]. Therefore, the  $\sqrt{B}$  dependence in Fig. 3 intensively implies again the characteristic property of 3D massless Dirac fermions in  $\text{ZrTe}_5$  under magnetic field.

In addition to the sequence of peaks at low field, the peak splitting shown in Fig. 1 could also be well resolved in Fig. 3. The  $n = 0$  peak evolves into four peaks at high magnetic field, with two very pronounced ones at lower energies and two relatively weak ones at higher energies. They are labeled as “1, 2, 3, 4” respectively in accordance with Fig. 1. The splittings of the rest peaks are, although too vague to be precisely identified, but for certain to exist. The  $n = 1$  peak, arising from transitions from  $L_{-2}$  to  $L_1$  and  $L_{-1}$  to  $L_2$ , seems to split into 3 peaks. Such splitting has never been observed in 2D massless Dirac fermion system, for example graphene[29].

We now explore the underlying mechanism for the splitting. We will show that this splitting can be naturally explained by the Zeeman effects of magnetic field on 3D Dirac fermions. The effect of Zeeman field on Dirac semimetals has been thoroughly studied by Burkov *et al.*[17]. It was pointed out that Zeeman field may split the Dirac node into two Weyl nodes, or transform the Dirac node into “line-nodes”[17]. Further including orbital effects of magnetic field will generate Zeeman-split Landau levels, schematically shown in Fig. 4. Here we will briefly explain the two possible scenarios and leave the details in the Supplementary Information[27].

The first scenario we consider is the “line-nodes” picture, with the resulting Landau level structure depicted in Fig. 4(a). The doubly degenerate Landau levels  $E_n(k_{\parallel})$  for  $n \neq 0$  from 3D Dirac fermions will be split into  $E_{n,\pm} \sim E_n(k_{\parallel}) \pm \bar{g}\mu_B B/2$ , where  $\bar{g}$  is the average Landé  $g$ -factor for the conduction and

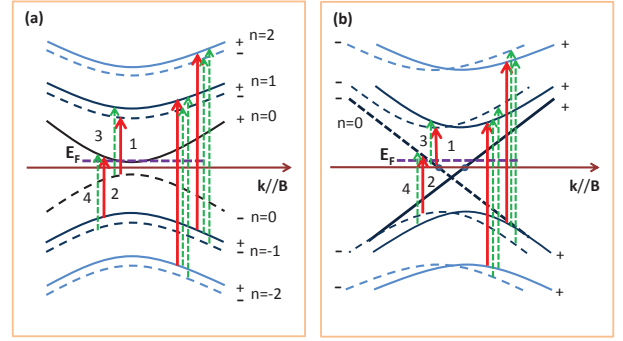


FIG. 4: Two proposed scenarios. The left panel (a) shows the splitting of Landau levels simply caused by Zeeman effect. The strong spin-orbit coupling could lead to a mixing of spin up and down components. So the split “+” (solid lines) and “-” (dashed lines) levels do not have pure spin up and spin down components. This would allow inter Landau level transitions to occur with opposite signs, however, weak in intensity. The purple dashed line is the Fermi energy  $E_F$ . Zeeman field without orbital effect will transform 3D Dirac node into “line-nodes” in this case[17]. The right panel (b) represents for the Landau levels of a Weyl semimetal induced by the magnetic field. The crossing points of  $n = 0$  Landau levels with the horizontal axis are the would-be Weyl points, if the orbital effect of magnetic field is ignored. The solid lines and dashed lines represent the two sets of Landau levels from the two Weyl nodes with opposite chirality. Transitions between Landau levels of opposite chirality will have weaker intensity. In both panels, the red solid arrows represent for transitions between Landau levels of the same spin/chirality, whereas the green dashed ones indicate that of different spin/chirality.

valence bands of 3D Dirac fermion. The  $n = 0$  Landau levels  $E_0(k_{\parallel}) = \pm \hbar v_{\parallel} k_{\parallel}$  will mix around  $k_{\parallel} = 0$  and open a gap of size  $\bar{g}\mu_B B$  there, and become  $E_{0,\pm} \sim \pm \sqrt{\hbar^2 v_{\parallel}^2 k_{\parallel}^2 + (\bar{g}\mu_B B/2)^2}$ . The split Landau levels are labeled by “spin” indices ‘+’ and ‘-’ in Fig. 4(a), which indicate that the states are of spin up or spin down at  $k_{\parallel} = 0$ . However with  $k_{\parallel} \neq 0$  the split Landau levels are not purely spin up or spin down due to strong spin-orbit coupling. Optical transitions between levels of the same “spin” indices can happen at  $k_{\parallel} = 0$ , and produce strong peaks in optical conductivity (thus reflectivity)[26], but transitions between levels of opposite spin indices will be suppressed at  $k_{\parallel} = 0$ , leading to weak and broad peaks. Therefore the original  $n = 0$  peak will split into two strong peaks “1” from  $L_{0,-}$  to  $L_{1,-}$ , and “2” from  $L_{-1,+}$  to  $L_{0,+}$ , and two weak peaks “3” from  $L_{0,-}$  to  $L_{1,+}$ , and “4” from  $L_{-1,-}$  to  $L_{0,+}$ . The peak “1” and peak “2” can have different energy if the chemical potential is not in the gap between  $L_{0,-}$  and  $L_{0,+}$  as depicted in Fig. 4(a), or if the conduction and valence bands of 3D Dirac fermion have different  $g$ -factor (see Supplementary Information[27]). In any case the splitting between peak “3” and peak “1”, and between peak “4” and peak “2” will be about  $\bar{g}\mu_B B$ . Based on previous *ab initio* results[22] on  $\text{ZrTe}_5$  and the experimental setup we conclude that this scenario is the most likely explanation of our observation (see Supplementary Information[27] for details).

The second and more interesting scenario is the “Weyl



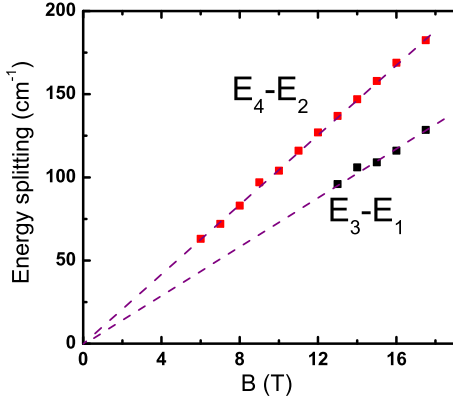


FIG. 5: The magnetic field dependent energy difference of  $E_3-E_1$  and  $E_4-E_2$ . They represent the Landau level splittings for the conduction and valence bands, respectively.

nodes” picture illustrated in Fig. 4(b). In this case the Zeeman field effectively shifts the wave vector parallel to field by  $\pm \tilde{g}\mu_B B/2\hbar v_{\parallel}$ , where the  $\pm$  sign depends on the chirality of Weyl fermions. The degenerate  $n \neq 0$  Landau levels become  $E_{n,\pm}(k_{\parallel}) \sim E_n(k_{\parallel} \mp \tilde{g}\mu_B B/2\hbar v_{\parallel})$ , and the  $n = 0$  Landau levels become  $E_{0,\pm}(k_{\parallel}) \sim \pm \hbar v_{\parallel} k_{\parallel} - \tilde{g}\mu_B B/2$ . In this scenario transitions between Landau levels of the same (different) chirality will have strong (weak) intensity. The original  $n = 0$  peak will also split into two strong peaks “1” from  $L_{0,-s}$  to  $L_{1,-s}$ , and “2” from  $L_{-1,-s}$  to  $L_{0,-s}$ , and two weak peaks “3” from  $L_{0,-s}$  to  $L_{1,s}$ , and “4” from  $L_{-1,s}$  to  $L_{0,-s}$ , where  $s = \pm$ . The peak “1” and peak “2” can have different energy if the chemical potential is not at the charge neutrality as depicted in Fig. 4(b). However the splitting between peak “3” and “1” will in general not be linear in  $B$ , unless the conduction and valence bands have very different  $g$ -factors. According to our analysis[27] this scenario is more likely to happen when the field is applied along crystal  $c$ -direction.

From the peak positions of “1”, “2”, “3” and “4”, we can immediately obtain the dependence of the split energy as a function of magnetic field. Figure 5 displays the magnetic field dependence of  $E_4 - E_2$  above 6 T and  $E_3 - E_1$  above 13 T, respectively. The energy positions for peak “3” could not be well resolved below 12 T, so the energy difference of  $E_3 - E_1$  is plotted only at high magnetic field. Obviously, both  $E_4 - E_2$  and  $E_3 - E_1$  exhibit good linear dependence, in better agreement with the first “line-nodes” scenario. The energy splitting is roughly  $10.5 \text{ cm}^{-1}/\text{T}$  ( $\sim 1.3 \text{ meV}/\text{T}$ ) for  $E_4 - E_2$  and  $7.4 \text{ cm}^{-1}/\text{T}$  ( $\sim 0.92 \text{ meV}/\text{T}$ ) for  $E_3 - E_1$ . According to previous discussions, this leads to estimates of the average  $g$ -factor being 22.5 or 15.8, from the  $E_4 - E_2$  or  $E_3 - E_1$  splittings respectively.

It was known that the  $g$ -factor reaches about 37 for  $\text{Cd}_3\text{As}_2$ [30], which is even bigger than our estimated  $g$ -factor for the  $\text{ZrTe}_5$  compound. We do not yet have a good explanation for the discrepancy between  $E_4 - E_2$  and  $E_3 - E_1$  splittings. Based on our analysis in Supplementary Information[27], this could be due to the broad nature of the weaker peaks, and the

current analysis may overestimate the  $g$ -factors for this reason.

The transitions associated with  $L_{-2} \rightarrow L_1$  and  $L_{-1} \rightarrow L_2$  are much more complex. Analogy to the transitions between  $L_0$  and  $L_{\pm 1}$ , the selection rule permissive ones (indicated by red solid arrows) should be more pronounced than those between opposite spin orientations (the dashed green ones). Considering possible different splittings of the valence and conduction bands, the  $n = 1$  peak appeared in  $R(B)/R(0)$  is supposed to contain at least three components.

In summary, by performing magneto-optical measurement on the single crystalline 3D massless Dirac semimetal  $\text{ZrTe}_5$ , we have clearly observed the magnetic field induced Landau levels, evidenced by regular organized peaks shown in the renormalized reflectivity  $R(B)/R(0)$ . Particularly, the first peak is identified to be originated from the transitions between the zeroth and first Landau Levels, which reveals the Fermi energy lies very close to the Dirac point. The appearance of the first peak under magnetic field as low as 1 T demonstrates an exceptionally low quantum limit of  $\text{ZrTe}_5$  compared to other 3D Dirac semimetals, which provided an elegant platform to explore more intriguing non-trivial quantum phenomena. Of most importance, the fourfold splitting of the first peak yield direct and clear evidence for the release of spin degeneracy of Landau level, hence the transformation from a Dirac semimetal into line-node or Weyl semimetal. Our theoretical modeling and analysis indicate that the former one is more likely realized in the present magnetic field configuration.

## ACKNOWLEDGMENTS

<sup>†</sup> These authors contributed equally to this work. We acknowledge very helpful discussions with Z. Fang, H. M. Weng, X. C. Xie, D. H. Lee, L. Fu, Q. Li, X. Dai, H. W. Liu. This work was supported by the National Science Foundation of China (11120101003, 11327806, 11374018), and the 973 project of the Ministry of Science and Technology of China (2011CB921701, 2012CB821403, 2014CB920902). Work at Brookhaven is supported by the Office of Basic Energy Sciences, Division of Materials Sciences and Engineering, U.S. Department of Energy under Contract No. DE-SC00112704.

\* Electronic address: wangfa@pku.edu.cn

<sup>†</sup> Electronic address: nlwang@pku.edu.cn

- [1] Z. Wang, Y. Sun, X.-Q. Chen, C. Franchini, G. Xu, H. Weng, X. Dai, and Z. Fang, Phys. Rev. B **85**, 195320 (2012), URL <http://link.aps.org/doi/10.1103/PhysRevB.85.195320>.
- [2] Z. Wang, H. Weng, Q. Wu, X. Dai, and Z. Fang, Phys. Rev. B **88**, 125427 (2013), URL <http://link.aps.org/doi/10.1103/PhysRevB.88.125427>.
- [3] X. Wan, A. M. Turner, A. Vishwanath, and S. Y. Savrasov, Phys. Rev. B **83**, 205101 (2011), URL <http://link.aps.org/doi/10.1103/PhysRevB.83.205101>.
- [4] Z. K. Liu, B. Zhou, Y. Zhang, Z. J. Wang, H. M. Weng, D. Prabhakaran, S.-K. Mo, Z. X. Shen,

- Z. Fang, X. Dai, et al., *Science* **343**, 864 (2014), <http://www.sciencemag.org/content/343/6173/864.full.pdf>, URL <http://www.sciencemag.org/content/343/6173/864.abstract>.
- [5] Z. K. Liu, J. Jiang, B. Zhou, Z. J. Wang, Y. Zhang, H. M. Weng, D. Prabhakaran, S.-K. Mo, H. Peng, P. Dudin, et al., *Nat. Mater.* **13**, 677 (2014), URL <http://dx.doi.org/10.1038/nmat3990>.
- [6] S. Borisenko, Q. Gibson, D. Evtushinsky, V. Zabolotnyy, B. Büchner, and R. J. Cava, *Phys. Rev. Lett.* **113**, 027603 (2014), URL <http://link.aps.org/doi/10.1103/PhysRevLett.113.027603>.
- [7] M. Neupane, S.-Y. Xu, R. Sankar, N. Alidoust, G. Bian, C. Liu, I. Belopolski, T.-R. Chang, H.-T. Jeng, H. Lin, et al., *Nat. Commun.* **5**, 3786 (2014), URL <http://dx.doi.org/10.1038/ncomms4786>.
- [8] S. M. Young, S. Zaheer, J. C. Y. Teo, C. L. Kane, E. J. Mele, and A. M. Rappe, *Phys. Rev. Lett.* **108**, 140405 (2012), URL <http://link.aps.org/doi/10.1103/PhysRevLett.108.140405>.
- [9] D. E. Kharzeev, *Prog. Part. Nucl. Phys.* **75**, 133 (2014), URL <http://www.sciencedirect.com/science/article/pii/S0146641014000839>.
- [10] L. P. He, X. C. Hong, J. K. Dong, J. Pan, Z. Zhang, J. Zhang, and S. Y. Li, *Phys. Rev. Lett.* **113**, 246402 (2014), URL <http://link.aps.org/doi/10.1103/PhysRevLett.113.246402>.
- [11] T. Liang, Q. Gibson, M. N. Ali, M. Liu, R. J. Cava, and N. P. Ong, *Nat. Mater.* **14**, 280 (2015), URL <http://dx.doi.org/10.1038/nmat4143>.
- [12] S.-Y. Xu, C. Liu, S. K. Kushwaha, R. Sankar, J. W. Krizan, I. Belopolski, M. Neupane, G. Bian, N. Alidoust, T.-R. Chang, et al., *Science* **347**, 294 (2015), <http://www.sciencemag.org/content/347/6219/294.full.pdf>, URL <http://www.sciencemag.org/content/347/6219/294.abstract>.
- [13] Y. Chen, S. Wu, and A. A. Burkov, *Phys. Rev. B* **88**, 125105 (2013), URL <http://link.aps.org/doi/10.1103/PhysRevB.88.125105>.
- [14] P. Hosur and X.-L. Qi, *Phys. Rev. B* **91**, 081106 (2015), URL <http://link.aps.org/doi/10.1103/PhysRevB.91.081106>.
- [15] A. C. Potter, I. Kimchi, and A. Vishwanath, *Nat. Commun.* **5**, 5161 (2014), URL <http://dx.doi.org/10.1038/ncomms6161>.
- [16] A. A. Burkov and L. Balents, *Phys. Rev. Lett.* **107**, 127205 (2011), URL <http://link.aps.org/doi/10.1103/PhysRevLett.107.127205>.
- [17] A. A. Burkov, M. D. Hook, and L. Balents, *Phys. Rev. B* **84**, 235126 (2011), URL <http://link.aps.org/doi/10.1103/PhysRevB.84.235126>.
- [18] E. V. Gorbar, V. A. Miransky, and I. A. Shnorkov, *Phys. Rev. B* **88**, 165105 (2013), URL <http://link.aps.org/doi/10.1103/PhysRevB.88.165105>.
- [19] M. Phillips and V. Aji, *Phys. Rev. B* **90**, 115111 (2014), URL <http://link.aps.org/doi/10.1103/PhysRevB.90.115111>.
- [20] A. Narayanan, M. D. Watson, S. F. Blake, N. Bruyant, L. Drigo, Y. L. Chen, D. Prabhakaran, B. Yan, C. Felser, T. Kong, et al., *Phys. Rev. Lett.* **114**, 117201 (2015), URL <http://link.aps.org/doi/10.1103/PhysRevLett.114.117201>.
- [21] J. Cao, S. Liang, C. Zhang, Y. Liu, J. Huang, Z. Jin, Z.-G. Chen, Z. Wang, Q. Wang, J. Zhao, et al. (2014), arXiv:1412.0824 (unpublished), URL <http://arxiv.org/abs/1412.0824>.
- [22] H. Weng, X. Dai, and Z. Fang, *Phys. Rev. X* **4**, 011002 (2014), URL <http://link.aps.org/doi/10.1103/PhysRevX.4.011002>.
- [23] Q. Li, D. E. Kharzeev, C. Zhang, Y. Huang, I. Pletikoscic, A. V. Fedorov, R. D. Zhong, J. A. Schneeloch, G. D. Gu, and T. Valla (2014), arXiv:1412.6543, URL <http://arxiv.org/abs/1412.6543>.
- [24] R. Y. Chen, S. J. Zhang, J. A. Schneeloch, C. Zhang, Q. Li, G. D. Gu, and N. L. Wang, *Phys. Rev. B* **92**, 075107 (2015), URL <http://link.aps.org/doi/10.1103/PhysRevB.92.075107>.
- [25] P. Hosur, S. A. Parameswaran, and A. Vishwanath, *Phys. Rev. Lett.* **108**, 046602 (2012), URL <http://link.aps.org/doi/10.1103/PhysRevLett.108.046602>.
- [26] P. E. C. Ashby and J. P. Carbotte, *Phys. Rev. B* **87**, 245131 (2013), URL <http://link.aps.org/doi/10.1103/PhysRevB.87.245131>.
- [27] Supplementary information.
- [28] M. Orlita, B. A. Piot, G. Martinez, N. K. S. Kumar, C. Faugeras, M. Potemski, C. Michel, E. M. Hankiewicz, T. Brauner, i. c. v. Drašar, et al., *Phys. Rev. Lett.* **114**, 186401 (2015), URL <http://link.aps.org/doi/10.1103/PhysRevLett.114.186401>.
- [29] M. L. Sadowski, G. Martinez, M. Potemski, C. Berger, and W. A. de Heer, *Phys. Rev. Lett.* **97**, 266405 (2006), URL <http://link.aps.org/doi/10.1103/PhysRevLett.97.266405>.
- [30] S. Jeon, B. B. Zhou, A. Gyenis, B. E. Feldman, I. Kimchi, A. C. Potter, Q. D. Gibson, R. J. Cava, A. Vishwanath, and A. Yazdani, *Nat. Mater.* **13**, 851 (2014), URL <http://dx.doi.org/10.1038/nmat4023>.